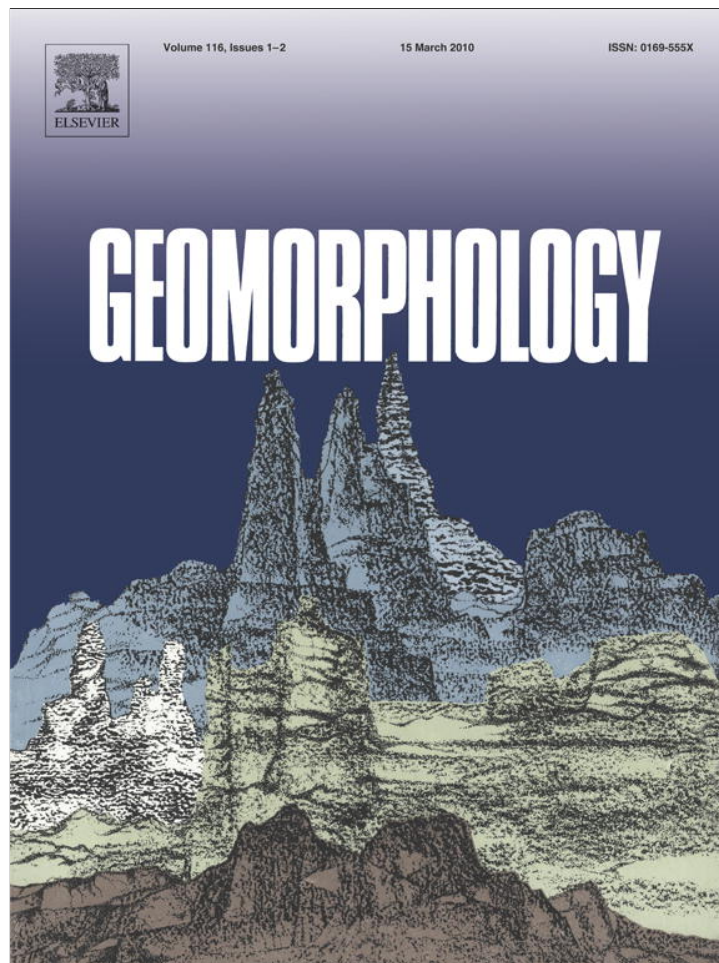


Provided for non-commercial research and education use.  
Not for reproduction, distribution or commercial use.



This article appeared in a journal published by Elsevier. The attached copy is furnished to the author for internal non-commercial research and education use, including for instruction at the authors institution and sharing with colleagues.

Other uses, including reproduction and distribution, or selling or licensing copies, or posting to personal, institutional or third party websites are prohibited.

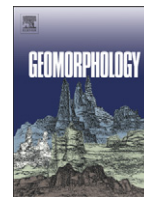
In most cases authors are permitted to post their version of the article (e.g. in Word or Tex form) to their personal website or institutional repository. Authors requiring further information regarding Elsevier's archiving and manuscript policies are encouraged to visit:

<http://www.elsevier.com/copyright>



Contents lists available at ScienceDirect

# Geomorphology

journal homepage: [www.elsevier.com/locate/geomorph](http://www.elsevier.com/locate/geomorph)

## Characterising spectral, spatial and morphometric properties of landslides for semi-automatic detection using object-oriented methods

Tapas R. Martha<sup>a,b,\*</sup>, Norman Kerle<sup>b</sup>, Victor Jetten<sup>b</sup>, Cees J. van Westen<sup>b</sup>, K. Vinod Kumar<sup>a</sup>

<sup>a</sup> National Remote Sensing Centre (NRSC), Indian Space Research Organisation (ISRO), Hyderabad-500625, India

<sup>b</sup> Department of Earth Systems Analysis, International Institute for Geo-Information Science and Earth Observation (ITC), Hengelosestraat 99, 7500 AA, Enschede, The Netherlands

### ARTICLE INFO

#### Article history:

Received 20 July 2009

Received in revised form 5 October 2009

Accepted 9 October 2009

Available online 17 October 2009

#### Keywords:

Landslide characterisation

Semi-automatic detection

Segmentation

Object-oriented analysis

The Himalayas

Disaster management

### ABSTRACT

Recognition and classification of landslides is a critical requirement in pre- and post-disaster hazard analysis. This has been primarily done through field mapping or manual image interpretation. However, image interpretation can also be done semi-automatically by creating a routine in object-based classification using the spectral, spatial and morphometric properties of landslides, and by incorporating expert knowledge. This is a difficult task since a fresh landslide has spectral properties that are nearly identical to those of other natural objects, such as river sand and rocky outcrops, and they also do not have unique shapes. This paper investigates the use of a combination of spectral, shape and contextual information to detect landslides. The algorithm is tested with a 5.8 m multispectral data from Resourcesat-1 and a 10 m digital terrain model generated from 2.5 m Cartosat-1 imagery for an area in the rugged Himalayas in India. It uses objects derived from the segmentation of a multispectral image as classifying units for object-oriented analysis. Spectral information together with shape and morphometric characteristics was used initially to separate landslides from false positives. Objects recognised as landslides were subsequently classified based on material type and movement as debris slides, debris flows and rock slides, using adjacency and morphometric criteria. They were further classified for their failure mechanism using terrain curvature. The procedure was developed for a training catchment and then applied without further modification on an independent catchment. A total of five landslide types were detected by this method with 76.4% recognition and 69.1% classification accuracies. This method detects landslides relatively quickly, and hence has the potential to aid risk analysis, disaster management and decision making processes in the aftermath of an earthquake or an extreme rainfall event.

© 2009 Elsevier B.V. All rights reserved.

### 1. Introduction

Landslides are a major natural hazard, causing significant damage to properties, lives and engineering projects in all mountainous areas in the world. According to a recent world report, approximately four million people were affected by landslides in 2006 (OFDA/CRED, 2006). Landslide hazard and risk management begins with comprehensive landslide detection/mapping, which serves as a basis to understand their spatial and temporal occurrences (Carrara and Merenda, 1976; Guzzetti et al., 2000; Brardinoni et al., 2003). Detection of landslides includes recognition and classification (Mantovani et al., 1996), frequently done using the systematic classification of landslides based on type of material and type of movement proposed by Varnes (1978). In Varnes' classification, the types of material are rock, debris and earth,

with falls, topples, slides, spreads and flows constituting movement types (Cruden and Varnes, 1996). The classification proposed by Varnes, and consistent with the UNESCO Working Party on the World Landslide Inventory (UNESCO-WP/WLI, 1993), is essentially a field based method, conceptualised and illustrated using block diagrams, without reference to their surrounding morphometry and contextual relationship. However, Earth observation data are increasingly used for landslide mapping, with automatic methods being preferable over manual approaches for obtaining quicker results over a large area, whereby the use of spectral, spatial, morphometric and contextual properties is essential to their success (Barlow et al., 2006; Borghuis et al., 2007). A comprehensive characterisation of landslides from an automatic detection perspective is required for the extraction of fast and accurate results that will help decision makers in implementing disaster management strategies.

Visual interpretation of aerial photographs, combined with field investigations, remained the major source for landslide inventory map preparation until recently (Kääb, 2002; Casson et al., 2003; van Westen and Lulie Getahun, 2003). Although aerial photographs accurately depict details of a landslide, they are often not available

\* Corresponding author. National Remote Sensing Centre (NRSC), Indian Space Research Organisation (ISRO), Hyderabad-500625, India. Tel.: +40 2388 4267; fax: +40 2377 2470.

E-mail addresses: [martha@itc.nl](mailto:martha@itc.nl), [tapas\\_martha@nrsdc.gov.in](mailto:tapas_martha@nrsdc.gov.in) (T.R. Martha).

in a timely manner for the majority of landslide prone areas in the world. Satellite imagery has become an alternative data source since it allows a more economic assessment of larger landslide affected areas, as well as a synoptic appreciation of the context within which landslides occur, especially in terms of land cover dynamics. Limited initially by low spatial resolution, early studies focused on pure detection of large landslides. However, recent studies have increasingly made use of very high resolution imagery (e.g. QuickBird, Ikonos, WorldView-1, Cartosat-1 and 2, SPOT-5 and ALOS-PRISM) for landslide mapping, and the number of operational sensors with similar characteristics is growing year by year (van Westen et al., 2008). Other remote sensing approaches of landslide inventory mapping, though infrequent, include shaded relief images produced from Light Detection and Ranging (LiDAR) and Synthetic Aperture Radar (SAR) interferometry based digital elevation models (DEMs) (Singhroy et al., 1998; Van Den Eeckhaut et al., 2007).

Preparation of landslide inventory maps using automatic methods has been attempted by previous researchers. Borghuis et al. (2007) showed how unsupervised classification could detect 63% of all landslides mapped manually. Other familiar automatic methods of landslide mapping are change detection and image fusion. Nichol and Wong (2005) showed the use of change detection technique to successfully differentiate landslides from spectrally similar features such as bare rock and soil. However, the automatic methods described above are pixel-based methods, and pixels are ill-suited to represent a geomorphic process such as a landslide. Therefore, the output gives 'salt and pepper' appearance, and are mostly not verifiable on the ground. These methods also rely only on the spectral signature, a property not unique for landslides. In addition to spectral signature, landslide diagnostic features can include vegetation, slope angle, slope morphology, drainage, tension cracks, presence of man-made features such as retaining walls, or artificial surface drainage. Previous researchers have attempted to quantify some of these landslide diagnostic features. Pike (1988) calculated the geometric signature from a DEM for a set of topographic variables that separates a landslide from its surroundings. Similarly, Iwahashi and Pike (2007) used slope gradient, terrain texture and local convexity derived from a DEM for automatic classification of topography. Previous works have also shown that an integration of remote sensing data and DEM derivatives produces a better result than the standalone approach (McDermid and Franklin, 1994; Florinsky, 1998). Object-oriented analysis (OOA), a platform for integration of different types of data (spectral, elevation and thematic), has already proven its ability for successful automatic classification of landforms (Dragut and Blaschke, 2006; van Asselen and Seijmonsbergen, 2006). It has a potential to detect landslides automatically in a better way than the pixel-based methods, by incorporating a multitude of landslide diagnostic features.

Object-oriented image classification is a knowledge driven method, whereby spectral, morphometric and contextual landslide diagnostic features can be integrated based on expert knowledge to accurately detect landslides (Barlow et al., 2003, 2006). Since landslides occur in diverse geomorphic settings, it is crucial to address a landslide as an object embedded in its surroundings. Image segmentation, a mandatory step prior to OOA does this by grouping spectrally homogenous pixels into an object (Batz and Schape, 2000). The significant advantage of OOA is the realistic outputs that can be easily verified on the ground. However, to make effective use of OOA, we need a comprehensive understanding of all potentially useful landslide characteristics, and specifically from a segmentation-based perspective. We also need to update and synthesize the criteria for the detection of landslides as per Varnes' classification scheme, using newer means of landslide inventory preparation, such as high resolution satellite data and DEMs. There have been limited attempts to detect landslides using OOA (e.g. Barlow et al., 2006). However, while they differentiated landslide types such as debris slides, debris flows and rock slides using OOA, their characterisation of different

landslide types is essentially data driven by considering a very limited set of parameters. In another recent study, Moine et al. (2009) used shape, spectral, texture and neighbourhood features, but no morphometric parameters, to detect landslides from aerial and satellite images using OOA. This clearly shows that the potential of OOA for automatic landslide detection has so far not been fully exploited. Using geomorphometry tools implemented in modern GIS softwares, and with the possibility of extracting many spectral, spatial and some morphometric parameters in image processing softwares, landslide characterisation can be done efficiently in comparison to tools available to previous researchers (e.g. Pike, 1988; McDermid and Franklin, 1994; Barlow et al., 2006), also creating possibilities for less data driven approaches.

The purpose of this paper is to update and synthesize the diagnostic features for semi-automatic detection (recognition and classification) of landslides, to provide an effective basis for researchers to develop object-based landslide mapping routines. The potential of spectral landslide diagnostic features such as normalised difference vegetation index (NDVI), shape features such as length/width ratios, asymmetry, texture, and morphometric features such as slope, terrain curvature and flow direction, derived from high resolution satellite data and a DEM, respectively, is discussed in this paper. OOA is effectively a combination of segmentation to derive image primitives, and their subsequent classification based on characteristics calculated from the extracted objects. This paper focuses primarily on object classification. In a separate study we address the segmentation and achievement of complex landslide shapes. Segmentation and extraction of spectral and texture characteristics were carried out using Definiens Developer software, while ArcGIS was used to derive additional morphometric indices. A complex analysis routine was then built in Definiens Developer to test how well all available spectral, textural, morphometric and contextual information can be used to detect landslides unambiguously. We test this routine in part of the High Himalayas that suffers extensively from landslides, and where efficient remote sensing data based techniques provide a real potential for improved landslide hazard and risk analysis.

## 2. Landslide characterisation from satellite data and a DEM

Characterisation of landslides and development of a knowledge base for their automatic detection are briefly discussed here. Image characteristics used for visual interpretation of landslides are equally important to the success of an automatic detection technique. Some of them, such as vegetation, drainage and morphology, were discussed by Soeters and van Westen (1996). The spectral characteristics based on digital number (DN) or NDVI values have been used by previous researchers for pixel-based methods of automatic detection of landslides (Nichol and Wong, 2005; Tarantino et al., 2007). To classify landslide types using object-based methods, Barlow et al. (2006) developed landslide diagnostic features using textural characteristics. However, they omitted one important parameter, morphometry, which is critical to distinguish commonly occurring landslide types: debris slides, debris flows and rock slides. Similarly, Moine et al. (2009) translated qualitative expert knowledge into quantitative criteria for characterising landslides using shape, spectral, texture and adjacency features. Although both studies made important contributions to object-based automatic detection landslides, failure mechanisms such as translational or rotational and their diagnostic features were not included. According to Varnes (1978), it is an important aspect of landslide studies when considering future hazard and ground stability analysis. Therefore, we discuss the following types of landslides based on their frequency of occurrence, and importance to landslide risk assessment. The discussion is illustrated with schematic block diagrams with emphasis on contextual and morphometric properties of landslide types (Fig. 1).

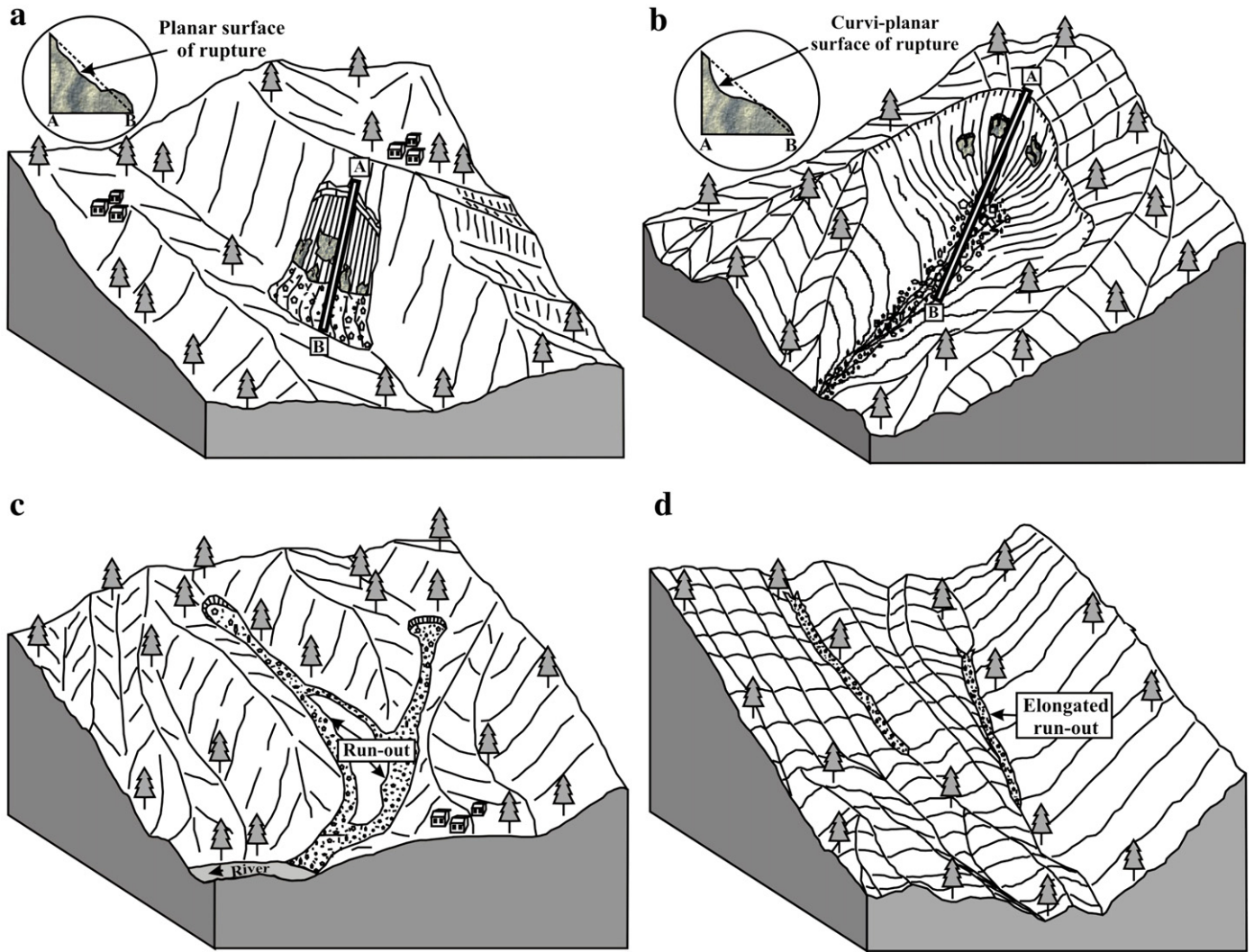


**Fig. 1.** Schematic block diagrams of landslide types. a) translational rock slide, b) rotational rock slide, c) debris flow, d) shallow translational rock slide. Debris slide is not shown separately since it has characteristics similar to debris flow, except less run-out.

### 2.1. Translational rock slide

Movement of rock down the slope along a planar or undulating surface of rupture (Cruden and Varnes, 1996). The value of terrain curvature is very low, sometimes close to zero. The source area is in a rock outcrop and slope is generally steep (Fig. 1a).

### 2.2. Rotational rock slide

Movement of rock down the slope along a curved and upwardly concave surface of rupture (Cruden and Varnes, 1996). It shows abrupt change in slope morphology, i.e. concavity in the zone of depletion and convexity in the zone of accumulation. The slope may be step-like due to backward tilting of slope facets (Soeters and van Westen, 1996). The crown shape is arcuate and located on or adjacent to the bed rock (Fig. 1b).

### 2.3. Debris flow

Spatially continuous movement of debris saturated with water (Cruden and Varnes, 1996). It generally has a moderate slope and large run-out, and a scouring effect is observed along the run-out path (Fig. 1c). The transition between slides to flows is gradual and depends on water content. Therefore, debris slides are characterised by a

limited run-out length. The source area can be in a deep zone of weathering, or topographic surface with large overburden depth.

### 2.4. Shallow translational rock slide

These landslides are surficial in nature and normally associated with first or second order drainage. They have generally very small width in comparison to length (Fig. 1d). Therefore, the length/width ratio is high and distance of the median line to the landslide periphery is very low.

## 3. Materials and methods

### 3.1. Study area

The Himalayas are one of the global hotspots for landslide hazard (Nadim et al., 2006). An area covering 81 km<sup>2</sup> in parts of the Mandakini river catchment in the High Himalayas around Okhimath town in the Uttarakhand state of India was selected for this study (Fig. 2). The extent of the study area was restricted to the watershed boundary. Although direct economic damage in this area is not as high as elsewhere in the world, the limited number of transport corridors, vital life lines for 208,000 people are frequently disrupted by landslides, seriously affecting the livelihoods and development of

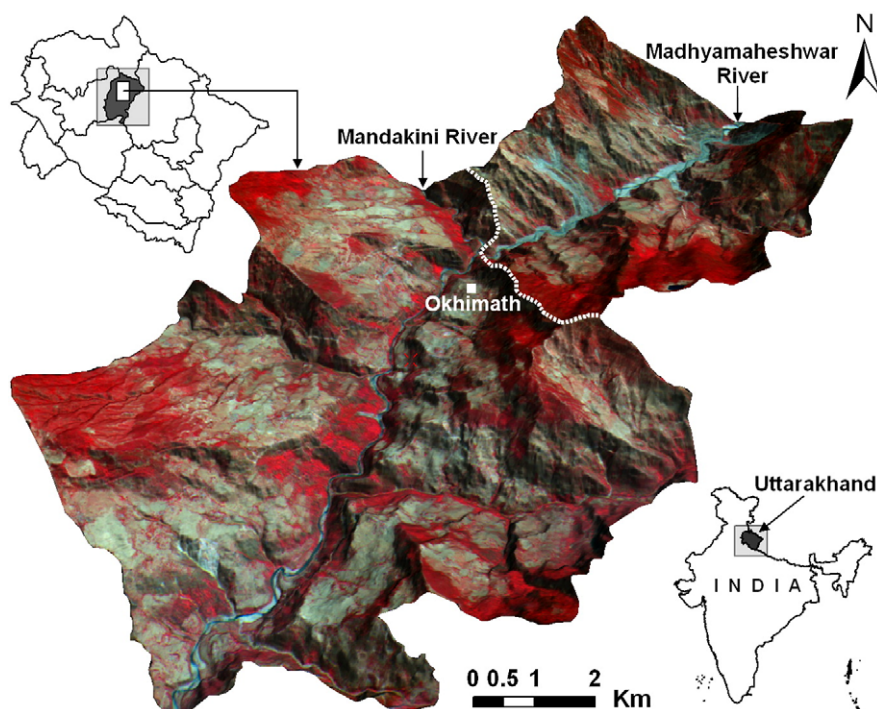


**Fig. 2.** Location map of the study area shown with a 3D perspective view. The white dotted line separates the Madhyamaheshwar sub-catchment in the north from the Mandakini catchment. (For interpretation of the references to colour in this figure legend, the reader is referred to the web version of this article.)

the people. Identification of landslide events and their types can be of use for more comprehensive landslide risk modeling and mitigation.

The Madhyamaheshwar river is a major tributary to the Mandakini river in this area. The elevation ranges between 867 and 2626 m with a high relative relief. Glacial landforms dominate this region, but are frequently modified by fluvial action. Some of the glacial landforms (e.g. moraines and solifluction lobes) with relatively gentle slopes have been converted into terraces for cultivation. Lithological units exposed in this area are granite gneisses, quartzite–sericite schist, quartzite, garnetiferous mica schist, marble and occasional basic intrusives (Rawat and Rawat, 1998). The foliations dip at moderate angles in NE to NNW directions. The main central thrust (MCT) dipping N to NE directions is the cause of neo-tectonic activity in this region, and has caused significant shearing of the rocks, rendering them vulnerable to landslides. The soil in this area is transported and composed of sub-angular rock fragments with a high proportion of sandy to sandy–silty matrix. However, small patches of silty and clayey soil, remnants of glacial deposit, are also present (Rawat and Rawat, 1998). The NE and SW parts of the study area are covered by evergreen oak forest.

This area offers a good opportunity to test the applicability of the semi-automatic detection technique, not only because of the occurrence of major and minor landslides, but also due to presence of different types of landslides associated with a variety of land covers. In August 1998, a total of 466 landslides triggered due to rainfall killed 103 people and damaged 47 villages in the Mandakini valley alone (Naithani, 2002). Some of these landslides were new, while others are as much as a century old but permanently active. The study area was divided into two parts, using a watershed divide, into the Madhyamaheshwar sub-catchment (28 km<sup>2</sup>) and the Mandakini catchment (53 km<sup>2</sup>). A landslide recognition and classification algorithm was developed for the Madhyamaheshwar sub-catchment and subsequently tested for the Mandakini catchment.

### 3.2. Data sources

#### 3.2.1. Satellite data

Steerable sensors and an increasing number of operational satellites have led to satellite data increasingly replacing aerial photo-

graphs for landslide studies. Multispectral data acquired on 16 April 2004 by Linear Imaging Self-scanning System IV (LISS-IV) sensor onboard the Indian Remote Sensing Satellite (IRS) P6 (also known as Resourcesat-1) were used for extracting the spectral diagnostic features. These data have been shown to be useful for mapping of major and minor landslides after the Kashmir earthquake in October, 2005 (Vinod Kumar et al., 2006). They have 5.8 m spatial resolution and three spectral bands viz. green (0.52 to 0.59  $\mu\text{m}$ ), red (0.62 to 0.68  $\mu\text{m}$ ) and near infra-red (0.76 to 0.86  $\mu\text{m}$ ). The Resourcesat-1 LISS-IV image was orthorectified using the 10 m DEM created from a 2.5 m resolution stereoscopic Cartosat-1 data acquired on 06 April 2006. The multispectral image was used to calculate the spectral characteristics of landslides, such as NDVI and brightness.

#### 3.2.2. DEM

Cartosat-1 carries two cameras, Pan-Aft and Pan-Fore with  $-5^\circ$  and  $+26^\circ$  view angles, respectively, and the data are provided with rational polynomial coefficients (RPCs) for block triangulation. High DEM accuracy is crucial for correctly quantifying the topographic parameters (Dewitte and Demoulin, 2005; Dragut and Blaschke, 2006). We used ground control points obtained from differential GPS (DGPS) surveys, to improve the orientation result of the RPC model during block/scene triangulation of Cartosat-1 data (Sadasiva Rao et al., 2006; Baltsavias et al., 2008), and could achieve a vertical root mean square error (RMSE) of 2.31 m. DEMs extracted automatically from aerial photographs/satellite images occasionally contain spurious spikes and pits (Kerle, 2002), although recent technical developments in photogrammetric processing, such as one implemented in the SAT-PP approach (Zhang and Gruen, 2006) used in our work, have reduced this problem. Photogrammetrically derived DEMs also reflect surface features such as vegetation and man-made objects, making them effectively digital surface models (DSMs). We used DEM editing tools in Leica Photogrammetric Suite (LPS) for manual height correction of isolated trees, while Erdas Imagine Stereo Analyst was used to estimate the average height of the scattered vegetation patches. Subsequently, the height of the vegetation patches was subtracted from the DSM to create a DEM. Elevation values from other potential

erroneous areas, such as shadows, were also corrected manually using breaklines. Finally, the DEM was hydrologically corrected using the FILL function of ArcGIS, and then derivatives such as slope, terrain curvature, hillshade and flow direction were calculated. These derivatives along with the DEM were used as input layers for OOA.

### 3.3. Segmentation technique

An important step before characterising diagnostic attributes of features of interest, such as landslides, is the creation of objects/segments that alone or in a group demarcate the boundary of the given feature. This is done using image segmentation, which is a process of dividing the image into objects or regions based on the homogeneity of the pixel values. Image segmentation can be done in different ways, using techniques such as density slicing, and split and merge (Kerle and de Leeuw, 2009). Our analysis was carried out in the Definiens Developer software environment, which has different types of algorithms for the image segmentation, multiresolution, quadtree and chessboard being the most efficient ones (Definiens, 2007). These algorithms can be combined effectively to obtain realistic and accurately classified outputs.

Landslides pose a particular challenge to segmentation, as land cover variability (e.g. partial vegetation), and illumination variations as a function of terrain characteristics, often result in spectrally diverse features. It is not practical to attempt outlining landslides as single segments, and some post-segmentation merging or multi-scale processing is needed also due to the typical size variability of landslides in an image. In this study, we initially attempted multiresolution segmentation, a process controlled by scale, shape, colour, compactness and smoothness parameters (Batz and Schape, 2000; Definiens, 2007), for delineating landslide candidate objects. After the assignment of a landslide class to qualified objects, we merged them for refinement of landslide object boundaries using a chessboard segmentation technique. OOA supports combining explicit and implicit feature identification, meaning that we can look for features for which unambiguous discriminators are known (explicit), but also remove background features that are not of interest (implicit), iteratively approaching an appropriate label of the sought features, such as landslides (Kerle and de Leeuw, 2009). Research on optimizing the use of OOA to achieve proper landslide segmentation, particularly with a spatial cluster analysis and multi-step segmentation technique, is carried out in a separate study. Once objects are appropriately outlined, Definiens Developer calculates a vast number of parameters for each derived object, such as layer mean, shape, texture, and relationship, based on the available data layers, to be used as class discriminators in OOA. In Definiens Developer, these attributes of image objects are referred to as object features (Definiens, 2007).

### 3.4. Approach for landslide recognition and classification

The approach for recognition and classification of landslides is mainly derived from the knowledge developed by experts for detection of landslides during image interpretation. It, therefore, mimics the cognitive approach a landslide expert would employ in visual image analysis. Fig. 3 shows the methodology adopted for the semi-automatic detection of landslides. The approach for landslide recognition and classification is described in the following three steps.

#### 3.4.1. Identification of landslide candidates (Step 1)

Bare rock or debris is exposed after a landslide event, giving a bright appearance to landslide affected areas in an image, although at times mixed with remaining or dislodged vegetation. This characteristic of a fresh landslide is very well captured by the remote sensing data and is used as a first criterion for recognition during visual image interpretation. This change to the land cover can be best represented in terms of NDVI, which is sensitive to low levels of vegetation cover.

NDVI has been successfully used by previous workers (Barlow et al., 2006; Schneevoigt et al., 2008) to discriminate landslides from vegetated features. Therefore, we used NDVI as a first criterion to identify landslide candidates, and separate them from other areas such as forest land, orchards and crop land.

#### 3.4.2. Separation of landslides from false positives (Step 2)

Since NDVI is used as a cut-off criterion, objects with similar or lower NDVI values, such as rock outcrops, roads, water bodies and river beds, are likely to be misclassified as landslides. In this step, these false positives are sequentially eliminated from the landslide class by integrating their spectral, morphometric and contextual information in OOA. Potential landslide false positives and the knowledge base for their classification are provided in Table 1, and the implementation of these criteria in Definiens Developer for OOA is described in Section 4.2.

#### 3.4.3. Identification of landslide types (Step 3)

The classification of landslides based on material and types of movement (Cruden and Varnes, 1996) was developed using the adjacency condition for source area. Morphometric criteria, quantified from Varnes' definition and local field knowledge, were used to classify landslides according to their failure mechanism. Shape criteria, such as length/width ratio and asymmetry (Barlow et al., 2006), were found to be useful for classifying shallow landslides. The knowledge base developed for classification of landslides from a semi-automatic detection perspective is explained in Table 2, and their implementation in Definiens Developer for OOA is described in Section 4.3.

## 4. Results

### 4.1. Extraction of landslide candidate objects

We carried out multiresolution image segmentation in Definiens Developer using Resourcesat-1 LISS-IV multispectral data for extracting landslide candidates. This process can be guided through the use of scale and shape parameters, the former being used to constrain maximum allowed heterogeneity in a segment. Given the natural landslide size and form variability, there is no single set of segmentation parameters that can delineate all landslide candidates accurately. Fig. 4 illustrates how sensitive the results are to parameter changes. In principle over-segmentation is preferred to under-segmentation, as later merging is possible, but small image features subsumed into a larger segment cannot be resolved later on. Therefore, a small scale factor, although leading to a large number of objects (Fig. 4b), was necessary to depict the relevant spectral, spatial and contextual properties of landslides.

Even though multiresolution segmentation initially produced sufficiently accurate landslide defining objects for analysis, they were occasionally found to contain impurities such as barren lands and small patches of vegetation. These landslide impurities were detected and removed by a resegmentation process, explained in Section 4.2.

### 4.2. Landslide recognition

An NDVI of 0.18, a value close to the statistical mode of the image NDVI, was found to be useful for discriminating landslide candidates from vegetation cover. From the landslide candidate class all false positives were sequentially eliminated using the criteria provided in Table 1, ultimately only retaining landslides. The classification sequence and the object features with their values used to classify the false positives are provided in Fig. 5. False positives such as shadow, river water bodies and roads, whose classification needs special attention, are explained below.

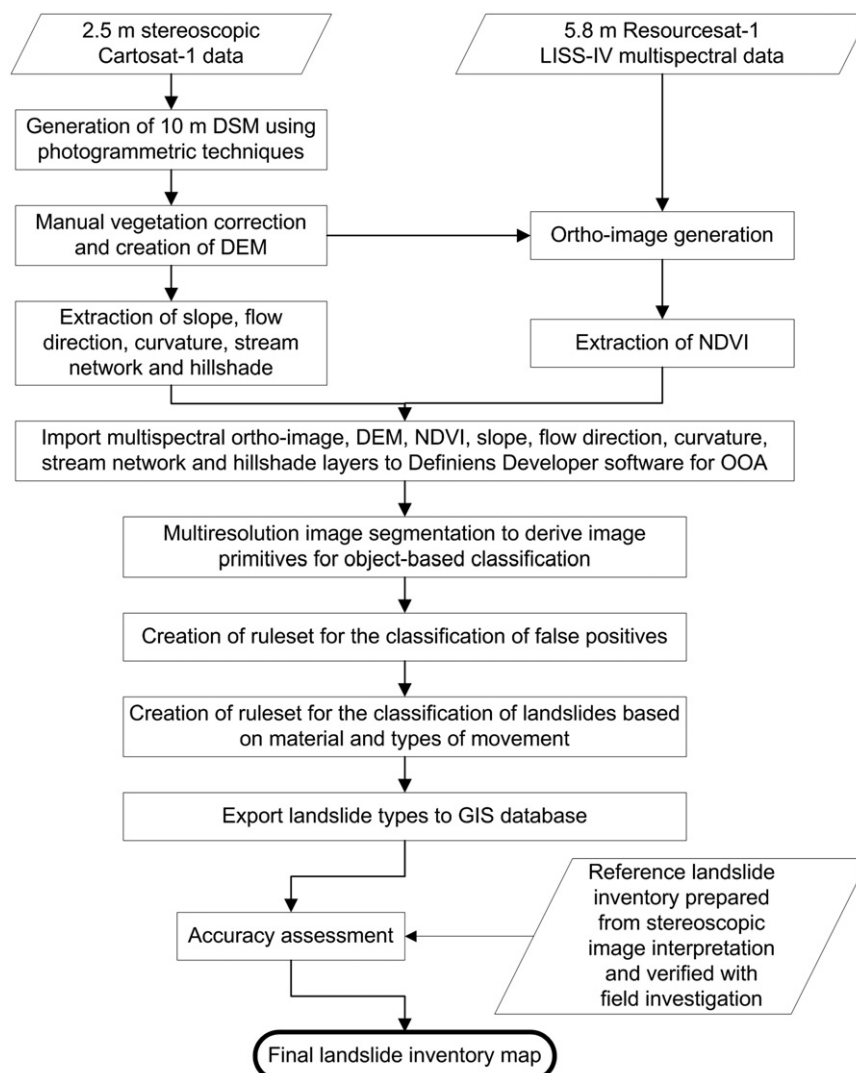


Fig. 3. Generalised methodology flowchart for semi-automatic detection of landslides using object-based methods.

Even though detection of shadow areas using the low brightness values from multispectral data is possible to some extent, a hillshade image is more reliable since other potential sources of low brightness such as water bodies and weathered rocks can be avoided. A hillshade image can be generated from a DEM, and it shows the surface illumination for a given position of sun by calculating the illumination values for each cell of the DEM. The position of sun, i.e. elevation and

azimuth, on the date of acquisition of multispectral image is provided by the data vendor in the file header.

Detection of water bodies, particularly the river water, was found to be difficult using the NIR band due to partial absorption of electro-magnetic radiation (EMR). This is because river water in the mountains flows at a high speed carrying suspended sediment load and mostly big boulders on the river bed are exposed above water

Table 1  
Landslide false positives and their logical classification criteria.

False positives	Criteria
Shadow	Hillshade, a hypothetical image created from a DEM for shadow condition using the sun position at the time of acquisition of the multispectral image, gives better information of shadow areas than lower DN values in the multispectral image.
Water body	Spectral information from the near infra-red (NIR) band, which shows lower values due to absorption of electro-magnetic radiation (EMR) by water. Topographic information, such as very gentle slope and adjacency to high order drainage carrying perennial flow of water, is also useful.
River sand	High brightness, gentle slope and low relief. Contextual information, such as adjacency to water bodies, is useful. Relief is used to differentiate it from debris flow, which also shows gentle slope, but high relief as the source area is in the mountains.
Built-up area	Large standard deviation values with neighbours (Navulur, 2007), typical texture due to the building pattern and gentle slope.
Non-rocky (e.g. agricultural land)	Low to moderate slope, low to moderate NDVI and typical texture due to the terraced pattern of topography.
Rocky (barren land)	Moderate slope (between 30° to 45°) and medium brightness.
Rocky (escarpment)	Steep slope (>45°) and medium brightness.
Road	Orientation is across the general flow direction. Contextual information such as high contrast to neighbours, e.g. roads within a forest in the mountains, is helpful.
Quarry	High brightness, and anomalous local depression due to excavation obtained from an up-to-date DEM. Contextual information, such as sudden truncation of road, is also useful.

**Table 2**  
Landslide types and their logical classification criteria.

Landslide type	Criteria
Shallow translational rock slide	Source area is in rocky land with shallow depth, and relatively narrow and elongated shape.
Debris slide	Source area is in a weathered zone or thickly covered soil, moderate slope and low length.
Debris flow	Source area is in a weathered zone or thickly covered soil and moderate slope, but has a long run-out zone.
Rotational rock slide	Source area is in rocky land with steep slopes, and terrain curvature is concave upward.
Translational rock slide	Source area is in rocky land with moderate slope and planar terrain curvature.

level, prohibiting complete absorption of EMR. Also, when a river flows in a deep gorge it is either covered by trees or topographic shadow. We, therefore, used the DEM to automatically derive the stream network and ordered them using the Strahler method (Strahler, 1965). This was used as an input thematic layer during OOA. In the study area, stream order 5th and beyond shows perennial flow of water. Therefore, only candidate objects intersecting such high order streams were assigned river water bodies class (Fig. 6). However, deep water bodies such as lakes were detected using low NIR values.

Moderate to gentle slopes in the study area are often converted to terraces for agricultural activity (Fig. 7). These terraces are parallel to contours, and width of such terraces is largely uniform. This feature of the terrace offers a unique texture in the image and can thus serve as a diagnostic feature. The frequency of combination of grey levels, i.e. texture in an image, is calculated using grey level co-occurrence matrix (GLCM), and in Definiens Developer software GLCM values are calculated using Haralick's method (Haralick et al., 1973). Mean GLCM of the red band discriminates the terrace pattern clearly and was thus used in combination with slope and NDVI to classify agricultural land in OOA (Fig. 5).

Flow direction is the direction of steepest descent, and roads are oriented perpendicular to flow (Fig. 8). Flow direction was derived from the DEM in ArcGIS using the *Dinf* (infinity direction) approach,

which calculates the flow in all possible directions and assigns a value in radians counter clockwise from east between 0 and  $2\pi$ , based on steepest slope on a triangular facet (Tarboton, 1997). The relatively orthogonal relationship between the flow direction and the main direction (longest axis direction) of false positives, combined with high length/width ratio was found to be extremely helpful for identification of roads (Fig. 8). Candidate objects with a main direction relatively parallel to the flow direction are classified as landslides.

Finally, a clean-up operation was performed to eliminate non-landslide areas occupying either all or parts of an object. First, an object, part of which was not landslide, was resegmented using a chessboard segmentation technique (Definiens, 2007) to produce small objects in a regular grid (Fig. 9a). Some of these small objects correspond to vegetation patches or rocky barren land, which could not be classified using the criteria discussed so far (Fig. 5), being part of a larger object. However, since now the object size is reduced, they were correctly classified using the same criteria as explained in Fig. 5. This left the objects fully misclassified as landslides to be eliminated (labels 'C' and 'D' in Fig. 9b). Definiens Developer provides an opportunity to search for additional criteria based on knowledge of the terrain, to refine the results. A careful observation of the image shows that the false positives were mostly river sands, either found along a tributary river (lower order stream) that flows seasonally, or in relatively high slope areas, which, therefore, could not be classified

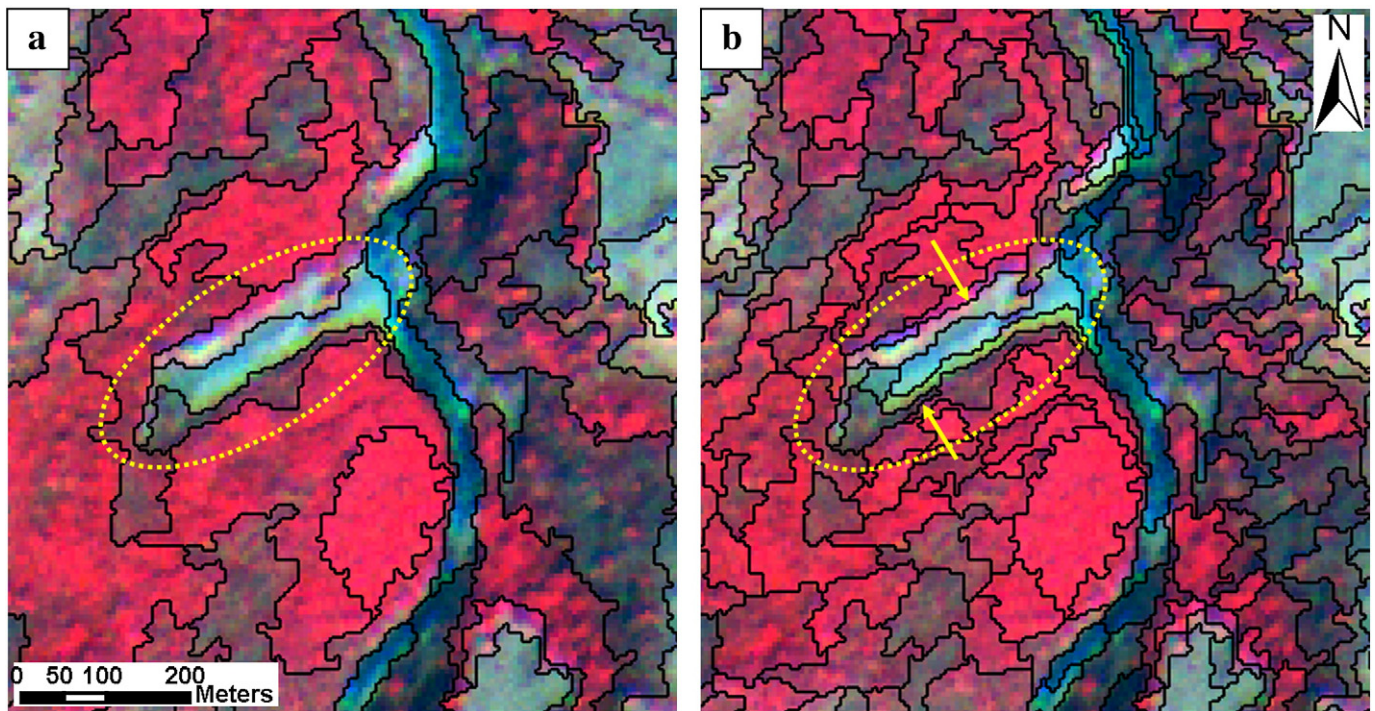


**Fig. 4.** Multiresolution segmentation of a Resourcesat-1 LISS-IV multispectral image. a) with scale parameter 30, the left and right flanks of the landslide (highlighted with dotted ellipse) are not correctly represented by image objects (with black outline). b) with scale parameter 10, objects are fully part of the landslide. Shape of 0.1 and compactness of 0.9 was used for both.

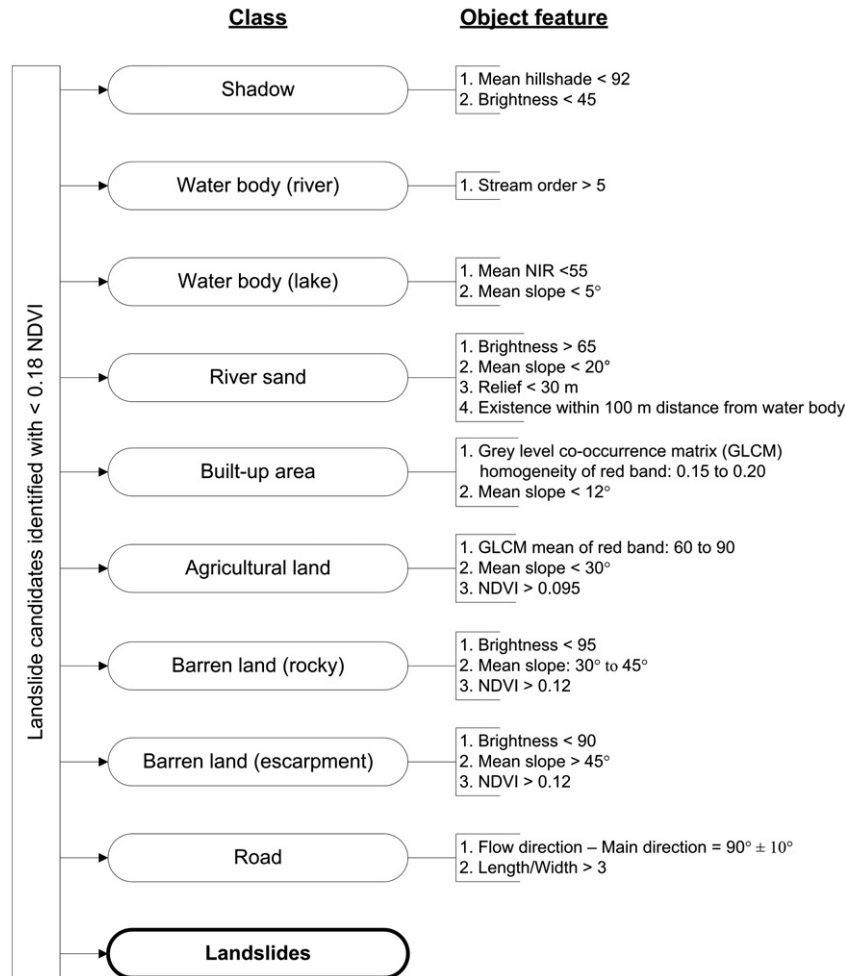


Fig. 5. Quantitative classification criteria for false positives. It also shows the sequence in which false positives were detected with top being attempted first. For acronyms, refer to text.

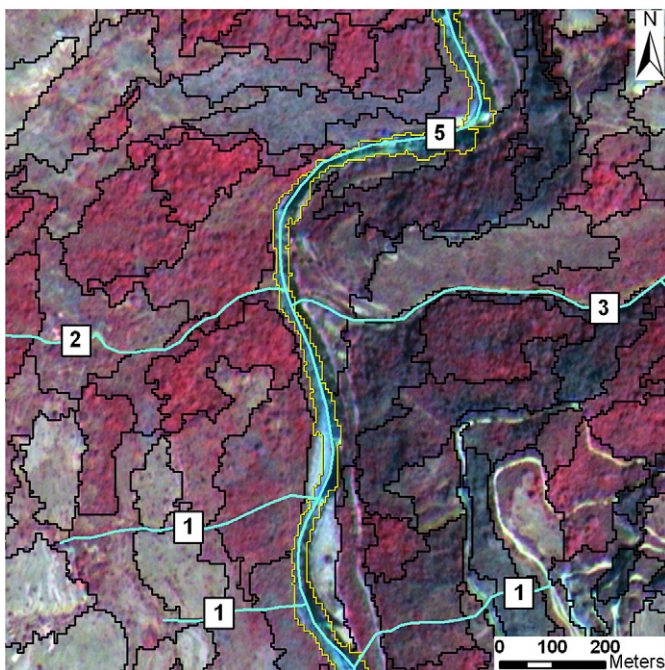


Fig. 6. Image object (yellow outline) identified as river water body using an automatically derived stream network. The numbers show the stream order. (For interpretation of the references to colour in this figure legend, the reader is referred to the web version of this article.)

due to non-fulfilment of the river sand criteria defined in Fig. 5. This issue was addressed using a merge option for the objects to redefine the object feature value, and by adding an asymmetry (ratio of the lengths of minor and major axes of an ellipse approximation of the object) condition to the original river sand criteria. Low relative relief of the objects calculated from the DEM was also useful in identifying river sands, particularly to differentiate it from debris flow deposits, which have a high relative relief due to the location of its source area at a high altitude in the valley (Fig. 5). Similarly, some other isolated misclassified landslides were classified as agricultural and rocky barren lands by refining their previous criteria. Thus only landslides were retained, ready to be classified based on type of material, type of movement and failure mechanism.

#### 4.3. Landslide classification

To apply diagnostic criteria for landslide classification, the small grids that resulted from chessboard segmentation (Fig. 9a) were merged (Fig. 9b). The recognised landslides were then classified by following a two-step approach. In the first step, the type of material was assigned to each landslide using contextual information, e.g. landslides adjacent to rocky land were classified as rock slides. Definiens Developer provides an opportunity to implement this knowledge (Table 2) by using ‘relative border to’ object feature (Fig. 10). The type of movement was assigned using shape criteria (Barlow et al., 2006), with landslides categorised as debris slides, debris flows or rock slides. Rock slides with shallow depth, which is inferred based on the narrow and elongated shape of the objects, were



Fig. 7. Field photograph of a typical agricultural terrace.

classified as shallow translational rock slides due to their prevalence in the study area and implication on future hazard analysis.

Classification of landslides based on the mechanism of failure, i.e. rotational or translational, requires segmentation and classification based on terrain curvature (Table 2). Therefore, in the second step, objects classified as debris slide and rock slide were resegmented by

multiresolution segmentation technique using the terrain curvature data instead of the multispectral data as done previously. Segmentation using curvature has an advantage that resulting objects reflect variation in concavity, convexity or planarity. Highly concave rupture surfaces thus indicate rotational failure, while planar rupture surfaces represent translational failure (Cruden and Varnes, 1996). The objects

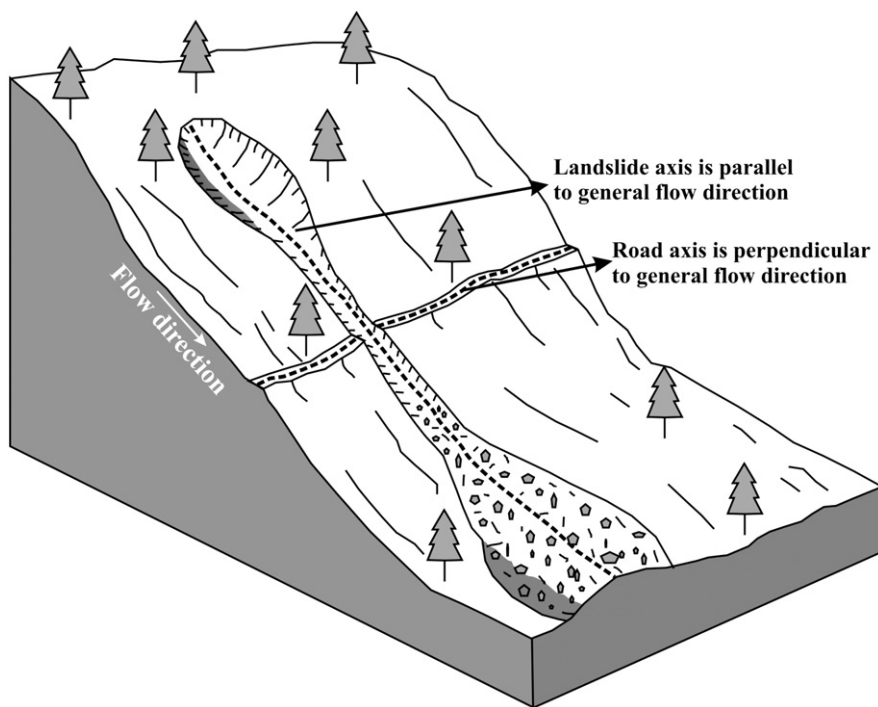
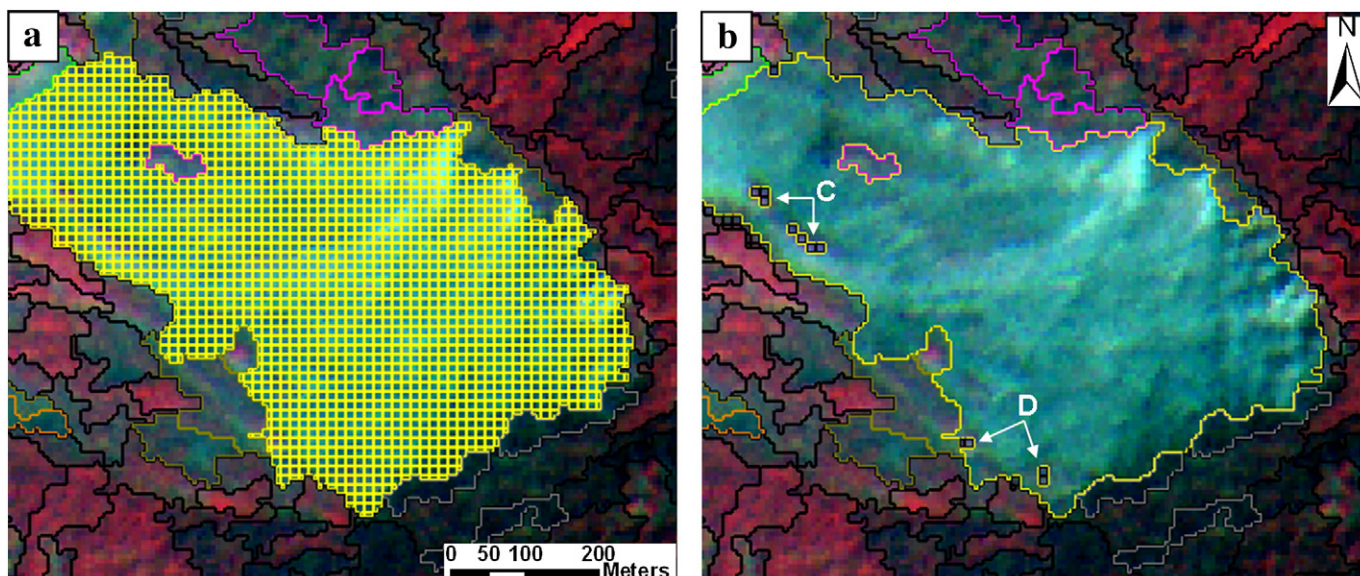


Fig. 8. Relationship between landslide and road object axes with reference to general flow direction.



**Fig. 9.** Resegmentation and merging of objects. a) chessboard segmentation to create small objects to eliminate small patches of vegetation or barren land (C and D in b) within bigger landslide objects. b) classification and removal of smaller patches and subsequent merging of the remaining gridded objects to a single landslide object for application of adjacency condition required for classification of landslides.

with mean curvature values less than  $-1$ , and between  $-1$  to  $+1$  are classified as rotational and translational rock slides, respectively (Fig. 10).

The algorithm (segmentation, recognition and classification) developed for the training area, i.e. the Madhyamaheshwar sub-catchment, was subsequently applied to the Mandakini catchment. All detected landslides were exported as a GIS layer for accuracy assessment. Fig. 11 shows the landslides recognised in the whole study area, varying in size between 774 and 291,591 m<sup>2</sup>.

#### 4.4. Accuracy assessment

In total 73 landslides were detected semi-automatically in the entire area. Accuracy assessment was carried out by comparing those against a manually prepared landslide inventory map. A detailed landslide inventory of the Okhimath area, including the watersheds analysed here, was prepared by Rawat and Rawat (1998) and Naithani (2002) after the occurrence of catastrophic landslides in August 1998. However, the inventory was not available in polygon shapes since they inventoried landslides by referring to the nearest village names. We used this

information and carried out a stereoscopic analysis of satellite data to prepare a landslide inventory map. The manually drawn landslide polygons were verified during detailed field investigation.

The accuracy of semi-automatically detected landslides was addressed on three levels: (i) number of correct recognition, (ii) correct classification of landslide types (Table 3), and (iii) correct detection of landslide extent (Table 4).

#### 5. Discussion

Landslide mapping by field investigations is a challenging task in vast and inaccessible mountainous terrain. Visual interpretation of remote sensing data is time consuming, and thus also not ideal, particularly for disaster management and decision making activities, where timely results are valued most. So far there have only been a few attempts at automating the mapping of landslides by pixel-based methods (Nichol and Wong, 2005), which likely fail as DN values alone do not characterise geomorphic processes such as landslide (McDermid and Franklin, 1994). Recently, Barlow et al. (2006) and Moine et al. (2009) started to investigate how landslides can be treated as objects in a contextual analysis. Barlow et al. (2006) achieved good detection accuracy by only considering landslides that are quite large ( $>10,000$  m<sup>2</sup>). Also, failure mechanisms, such as rotational and translational, are not addressed by them. However, Moine et al. (2009) could recognise small landslides, essentially using high resolution earth observation data, but did not use a DEM, eventually ruling out the possibilities of classifying landslide types. Use of expert knowledge to characterise landslides is crucial for semi-automatic detection in OOA. This was addressed partly by Moine et al. (2009), whereas Barlow et al. (2006) used supervised classification with object samples to classify landslide candidates. Therefore, a proper characterisation of landslide types is required for OOA. In this study we extracted objects from segmentation of high resolution (5.8 m) Resourcesat-1 LISS-IV multispectral data and a 10 m Cartosat-1 derived DEM, and characterised major landslide types as per Varnes' classification scheme.

A multi-step segmentation approach was followed to recognise and classify landslides accurately. Expert knowledge was quantified using spectral characteristics of the objects such as layer mean and brightness, morphometric characteristics such as flow direction, slope and curvature, shape characteristics such as asymmetry and the

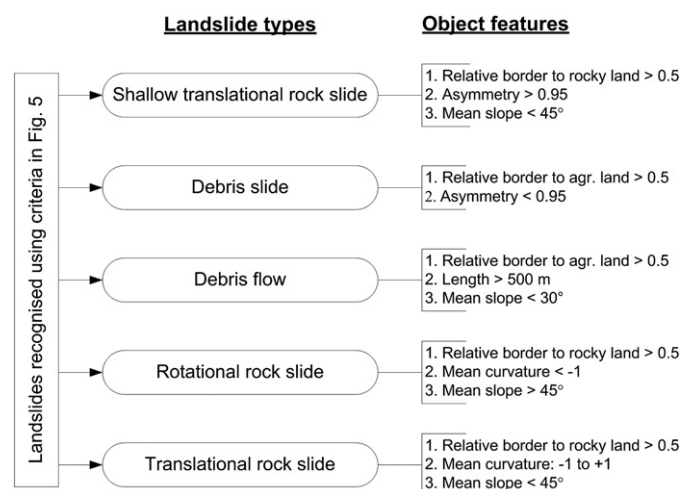


**Fig. 10.** Quantitative classification criteria for landslide types. It also shows the sequence in which the landslides were classified with top being attempted first.

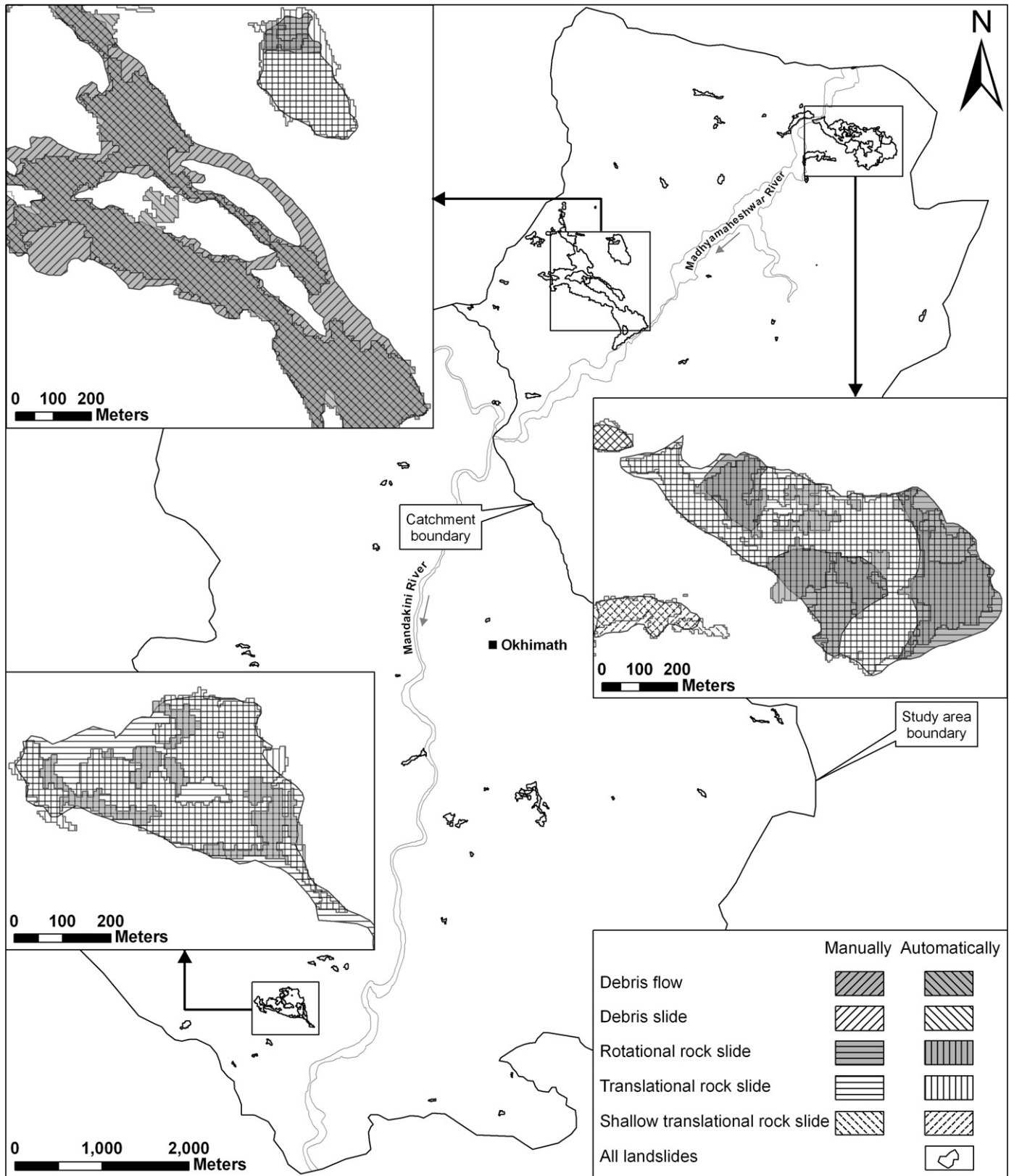


Fig. 11. Landslides semi-automatically detected for the whole study area (black polygons). Three insets show the extent of major landslides detected automatically. Landslides mapped manually by visual image interpretation are shown in the background for comparison. Intersection of line symbols shows agreement.

length/width ratio, textural characteristics such as GLCM (Haralick et al., 1973), and contextual information such as adjacency and containment, to classify a total of nine false positive classes (Fig. 5). A

stream network automatically derived from a DEM was helpful in delineating river water body with ambiguous spectral properties. GLCM texture and orthogonal relationship between flow and main

**Table 3**  
Accuracy assessment for the number of landslides.

	Landslide detection					
	Manually	Automatically				
		LCRC	LCRWC	TLCR	LNR	LOR
Shallow translational rock slide	31	16	4	20	11	2
Debris flow	1	1	0	1	0	0
Debris slide	4	3	0	3	1	17
Rotational rock slide	6	6	0	6	0	3
Translational rock slide	13	12	0	12	1	9
Total number of landslides	55	38	4	42	13	31
%		69.1	7.3	76.4	23.6	56.4

LCRC: Landslides correctly recognised and classified, LCRWC: Landslides correctly recognised but wrongly classified, TLCR: Total landslides correctly recognised (LCRC + LCRWC), LNR: Landslides not recognised (i.e. error of omission), LOR: Landslides over recognised (i.e. error of commission).

directions of objects were useful for classification of agricultural terraces and roads, respectively. Classification of false positives into non-rocky and rocky lands was useful in classifying landslides based on material type. This study thus considers generic indicators based on expert knowledge to characterise landslides. However, the quantification of specific characteristic features may have to be adjusted, when our algorithm is applied to other areas or used with other image data types.

Merging and resegmentation in Definiens Developer during OOA provided an ideal solution for detecting not only landslides of complex shape and size, but also landslides with multiple failure mechanisms, e.g. rotational and translational, within a landslide body. Multiresolution segmentation used for the creation of landslide candidate objects, and subsequent chessboard segmentation, successfully eliminated smaller patches of vegetation or barren land, which later proved essential for refinement of landslide boundaries. Segmentation of landslide objects using terrain curvature data was able to classify landslides based on their failure mechanism.

We achieved 76.4% recognition and 69.1% classification accuracies for the whole study area in terms of number of landslides (Table 3). The recognition and classification accuracies achieved for the extent of landslides are 69.9% and 69.5%, respectively, and 23.6% of the total number of landslides and 3.7% of corresponding extent could not be recognised (Table 4). Shallow translational rock slides were recognised and classified with lower accuracy than other four types (Table 3). The reason for non-detection of 11 shallow translational rock slides was incorrect delineation of appropriate objects in the segmentation routine, due to their narrow shape and occurrence within spectrally identical land cover units, such as rocky land. Even

**Table 4**  
Accuracy assessment for the extent (km<sup>2</sup>) of landslides.

	Landslide detection					
	Manually	Automatically				
		LCRC	LCRWC	TLCR	LNR	LOR
Shallow translational rock slide	0.220	0.103	0.005	0.108	0.039	0.007
Debris flow	0.387	0.292	0	0.292	0	0
Debris slide	0.052	0.029	0	0.029	0.003	0.043
Rotational rock slide	0.162	0.098	0	0.098	0	0.035
Translational rock slide	0.379	0.312	0	0.312	0.003	0.026
Total extent of landslide	1.200	0.834	0.005	0.839	0.045	0.111
%		69.5	0.4	69.9	3.7	9.2

LCRC: Landslides correctly recognised and classified, LCRWC: Landslides correctly recognised but wrongly classified, TLCR: Total landslides correctly recognised (LCRC + LCRWC), LNR: Landslides not recognised (i.e. error of omission), LOR: Landslides over recognised (i.e. error of commission).

though the number of identified debris slides was too high (17), their extent is small. These wrongly classified debris slides are actually parts of agricultural land, showing a mixed spectral response owing to their partial conversion to built-up area.

The smallest landslide correctly detected by our algorithm is 774 m<sup>2</sup>. However, to understand the detection capability of our algorithm in relation to landslide size, we applied the landslide frequency–size distribution analysis, a proven technique for landslide inventory assessment (Malamud et al., 2004). Manually (55) and automatically (42) recognised landslides were plotted against their frequencies (Fig. 12). Since the range of landslide size is very high, we selected a logarithmic class interval (x-axis). As the class interval is not constant, we also normalised the frequency with their respective class interval to calculate the probability density (Malamud et al., 2004) and plotted it on the y-axis. Both trend lines showed good statistical correlations, meaning that the data resolution and algorithm are sufficient to accurately recognise the most commonly occurring landslide sizes.

## 6. Conclusions

In this study landslides were semi-automatically recognised and classified as per Varnes' classification scheme. Landslide diagnostic features typically used by experts during visual image interpretation were used for the characterisation. These characteristic features were updated from an automatic detection perspective, and then efficiently synthesized using OOA for recognition and classification of landslides.

The algorithm was developed in Definiens Developer software using only two primary data sources, high resolution satellite data and a DEM. It comprised 45 individual routines, such as segmentation, merging and classification, which are automatically executed in the assigned sequence. Other parameters used, such as NDVI, slope, flow direction, hillshade, terrain curvature and stream network were derived automatically using algorithms available in basic GIS and image processing softwares. Landslide candidate objects, once identified in the segmentation routine were separated from vegetation by an NDVI threshold. Nine false positive classes were effectively removed by efficient use of DEM derivatives combined with spectral information. For the entire study area, we achieved 76.4% landslide recognition accuracy in five different landslide classes in a terrain featuring spectrally identical land use/cover units. It must also be noted that correct visual identification of these types based on image data alone would be very challenging and would also require the incorporation of elevation information. For example, the smallest

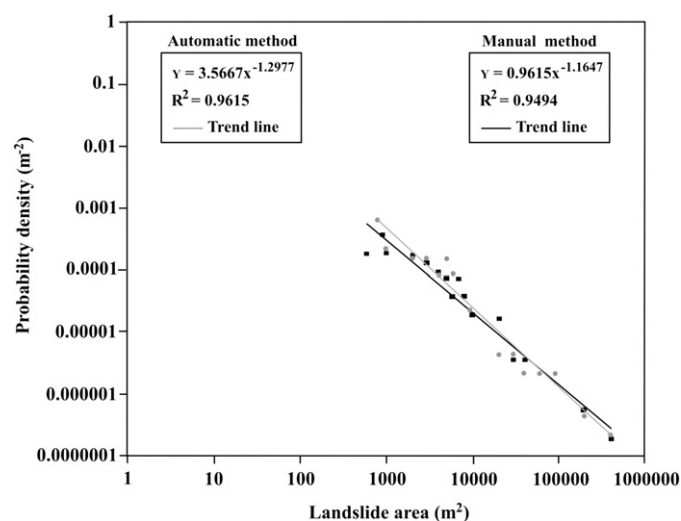


Fig. 12. Relationship between landslide area and frequency.

automatically detected landslide (774 m<sup>2</sup>) was missed in the visual stereo interpretation, and only verified with higher resolution Google Earth imagery. Another significant achievement of this study is detection of complex failure mechanism within large landslides. Since the algorithm uses NDVI in the beginning to identify landslide candidates, the result of the OOA, in principle, will be accurate if the post-landslide satellite imagery and DEM are used. Therefore, our method has the potential to produce quick results after an earthquake or an extreme rainfall event. Also, since the algorithm could distinguish between rotational and translational slides, future hazard analysis and immediate ground control measures can be planned efficiently (Varnes, 1978).

The objective here was to evaluate to what extent landslides, once outlined in a (possibly iterative or multi-stage) segmentation routine, can be correctly detected, using an OOA. The challenge of segmenting complex landslide shapes, which are frequently distorted as a result of sensor and viewing characteristics, and which become indistinct when shadows overlap or contrast is low, will be addressed in a separate study. The algorithm developed here is available on our website ([www.itc.nl/OOA-group](http://www.itc.nl/OOA-group)), and we welcome testing of the approach with other data types and in other areas.

### Acknowledgements

This paper is the outcome of the research carried out under the framework of GSI-NRSC-ITC joint collaboration. The support by the Director, NRSC and Dr. P.S. Roy, Deputy Director, RS&GIS-AA, NRSC is duly acknowledged. The research is carried out as part of the United Nations University–ITC School for Disaster Geo-Information Management ([www.itc.nl/unu/dgim](http://www.itc.nl/unu/dgim)).

### References

- Baatz, M., Schape, A., 2000. Multiresolution segmentation: an optimization approach for high quality multi-scale image segmentation. In: Strobl, L.J., Blaschke, T., Griesebener, T. (Eds.), *Angewandte geographische informationsverarbeitung XII, Beiträge zum AGIT Symposium Salzburg 2000*. Herbert Wichmann Verlag, Heidelberg, pp. 12–23.
- Baltsavias, E., Kocaman, S., Wolff, K., 2008. Analysis of Cartosat-1 images regarding image quality, 3D point measurement and DSM generation. *The Photogrammetric Record* 23, 305–322.
- Barlow, J., Martin, Y., Franklin, S.E., 2003. Detecting translational landslide scars using segmentation of Landsat ETM+ and DEM data in the northern Cascade Mountains, British Columbia. *Canadian Journal of Remote Sensing* 29, 510–517.
- Barlow, J., Franklin, S., Martin, Y., 2006. High spatial resolution satellite imagery, DEM derivatives, and image segmentation for the detection of mass wasting processes. *Photogrammetric Engineering and Remote Sensing* 72, 687–692.
- Borghuis, A.M., Chang, K., Lee, H.Y., 2007. Comparison between automated and manual mapping of typhoon-triggered landslides from SPOT-5 imagery. *International Journal of Remote Sensing* 28, 1843–1856.
- Brardinoni, F., Slaymaker, O., Hassan, M.A., 2003. Landslide inventory in a rugged forested watershed: a comparison between air-photo and field survey data. *Geomorphology* 54, 179–196.
- Carrara, A., Merenda, L., 1976. Landslide inventory in northern Calabria, southern Italy. *Geological Society of America Bulletin* 87, 1153–1162.
- Casson, B., Delacourt, C., Baratoux, D., Allemand, P., 2003. Seventeen years of the “La Clapiere” landslide evolution analysed from ortho-rectified aerial photographs. *Engineering Geology* 68, 123–139.
- Cruden, D., Varnes, D.J., 1996. Landslide types and processes. In: Turner, A.K., Schuster, R.L. (Eds.), *Landslides Investigation and Mitigation*. : Special Report, 247. Transportation Research Board, National Academy of Sciences, Washington D.C, pp. 36–75.
- Definiens, 2007. Developer 7: Userguide. Definiens Imaging GmbH.
- Dewitte, O., Demoulin, A., 2005. Morphometry and kinematics of landslides inferred from precise DTMs in West Belgium. *Natural Hazards and Earth System Sciences* 5, 259–265.
- Dragut, L., Blaschke, T., 2006. Automated classification of landform elements using object-based image analysis. *Geomorphology* 81, 330–344.
- Florinsky, I.V., 1998. Combined analysis of digital terrain models and remote sensing data in landscape investigations. *Progress in Physical Geography* 22, 33–60.
- Guzzetti, F., Cardinali, M., Reichenbach, P., Carrara, A., 2000. Comparing landslide maps: a case study in the upper Tiber River Basin, central Italy. *Environmental Management* 25, 247–263.
- Haralick, R., Shanmugam, K., Itshak, D., 1973. Textural features for image classification. *IEEE Transactions on Systems, Man, and Cybernetics* 6, 610–621.
- Iwahashi, J., Pike, R.J., 2007. Automated classifications of topography from DEMs by an unsupervised nested-means algorithm and a three-part geometric signature. *Geomorphology* 86, 409–440.
- Kääb, A., 2002. Monitoring high-mountain terrain deformation from repeated air- and spaceborne optical data: examples using digital aerial imagery and ASTER data. *ISPRS Journal of Photogrammetry and Remote Sensing* 57, 39–52.
- Kerle, N., 2002. Volume estimation of the 1998 flank collapse at Casita volcano, Nicaragua: a comparison of photogrammetric and conventional techniques. *Earth Surface Processes and Landforms* 27, 759–772.
- Kerle, N., de Leeuw, J., 2009. Reviving legacy population maps with object-oriented image processing techniques. *IEEE Transactions on Geoscience and Remote Sensing* 47, 2392–2402.
- Malamud, B.D., Turcotte, D.L., Guzzetti, F., Reichenbach, P., 2004. Landslide inventories and their statistical properties. *Earth Surface Processes and Landforms* 29, 687–711.
- Mantovani, F., Soeters, R., van Westen, C.J., 1996. Remote sensing techniques for landslide studies and hazard zonation in Europe. *Geomorphology* 15, 213–225.
- McDermid, G.J., Franklin, S.E., 1994. Spectral, spatial, and geomorphometric variables for the remote sensing of slope processes. *Remote Sensing of Environment* 49, 57–71.
- Moine, M., Puissant, A., Malet, J.-P., 2009. Detection of landslides from aerial and satellite images with a semi-automatic method. Application to the Barcelonnette basin (Alpes-de-Haute-Provence, France). In: Malet, J.-P., Rémaitre, A., Bogaard, T. (Eds.), *Landslide Processes: From Geomorphological Mapping to Dynamic Modelling*. CERG, Strasbourg, France, pp. 63–68.
- Nadim, F., Kjekstad, O., Peduzzi, P., Herold, C., Jaedicke, C., 2006. Global landslide and avalanche hotspots. *Landslides* 3, 159–173.
- Naithani, A.K., 2002. The August, 1998 Okhmath tragedy in Rudraprayag district of Garhwal Himalaya, Uttaranchal, India. *GIA* 16, 145–156.
- Navulur, K., 2007. *Multispectral image analysis using the object-oriented paradigm*. CRC, Boca Raton. 165 pp.
- Nichol, J., Wong, M.S., 2005. Satellite remote sensing for detailed landslide inventories using change detection and image fusion. *International Journal of Remote Sensing* 26, 1913–1926.
- OFDA/CRED, 2006. EM-DAT International Disaster Database - [www.em-dat.net](http://www.em-dat.net). Université Catholique de Louvain, Brussels, Belgium.
- Pike, R.J., 1988. The geometric signature: quantifying landslide-terrain types from digital elevation models. *Mathematical Geology* 20, 491–511.
- Rawat, U.S., Rawat, J.S., 1998. A report on geotechnical reconnaissance of the excessive landsliding in August, 1998 near Okhmath, Rudraprayag district, U.P. Technical report. Geological Survey of India, Northern Region, Lucknow.
- Sadasiva Rao, B., Murali Mohan, A.S.R.K.V., Kalyanaraman, K., Radhakrishnan, K., 2006. Evaluation of Cartosat-1 Stereo Data of Rome. International Symposium on Geospatial Databases for Sustainable Development, International Symposium on Geospatial Databases for Sustainable Development, ISPRS TC-IV.
- Schneevoigt, N.J., van der Linden, S., Thamm, H.-P., Schrott, L., 2008. Detecting Alpine landforms from remotely sensed imagery. A pilot study in the Bavarian Alps. *Geomorphology* 93, 104–119.
- Singhroy, V., Mattar, K.E., Gray, A.L., 1998. Landslide characterisation in Canada using interferometric SAR and combined SAR and TM images. *Advances in Space Research* 21, 465–476.
- Soeters, R., van Westen, C.J., 1996. Slope instability. Recognition, analysis and zonation. In: Turner, A.K., Schuster, R.L. (Eds.), *Landslide: Investigations and Mitigation*. Special Report 247. Transportation Research Board, National Academy of Sciences, Washington D.C, pp. 129–177.
- Strahler, A.N., 1965. *Introduction to Physical Geography*. Wiley & Sons, New York.
- Tarantino, C., Blonda, P., Pasquariello, G., 2007. Remote sensed data for automatic detection of land-use changes due to human activity in support to landslide studies. *Natural Hazards* 41, 245–267.
- Tarboton, D.G., 1997. A new method for the determination of flow directions and contributing areas in grid digital elevation models. *Water Resources Research* 33, 309–319.
- UNESCO-WP/WLI, 1993. *Multilingual Landslide Glossary*. Bitech Publishers Ltd, Richmond. 34 pp.
- van Asselen, S., Seijmonsbergen, A.C., 2006. Expert-driven semi-automated geomorphological mapping for a mountainous area using a laser DTM. *Geomorphology* 78, 309–320.
- Van Den Eckhaut, M., et al., 2007. Use of LIDAR-derived images for mapping old landslides under forest. *Earth Surface Processes and Landforms* 32, 754–769.
- van Westen, C.J., Castellanos, E., Kuriakose, S.L., 2008. Spatial data for landslide susceptibility, hazard, and vulnerability assessment: an overview. *Engineering Geology* 102, 112–131.
- van Westen, C.J., Lulie Getahun, F., 2003. Analyzing the evolution of the Tessina landslide using aerial photographs and digital elevation models. *Geomorphology* 54, 77–89.
- Varnes, D.J., 1978. Slope movements types and processes. In: Schuster, R.L., Krizek, R.L. (Eds.), *Landslides: Analysis and Control*. Special Report 176. Transportation Research Board, National Academy of Sciences, Washington D.C, pp. 11–33.
- Vinod Kumar, K., Martha, T.R., Roy, P.S., 2006. Mapping damage in the Jammu and Kashmir caused by 8 October 2005 Mw 7.3 earthquake from the Cartosat-1 and Resourcesat-1 imagery. *International Journal of Remote Sensing* 27, 4449–4459.
- Zhang, L., Gruen, A., 2006. Multi-image matching for DSM generation from IKONOS imagery. *ISPRS Journal of Photogrammetry and Remote Sensing* 60, 195–211.